catalysts

MDPI

Article

Production of Bio-Oil from Sugarcane Bagasse through Hydrothermal Liquefaction Processes with Modified Zeolite Socony Mobil-5 Catalyst

Thandiswa Jideani [1], Ntalane Sello Seroka [1,2,*] and Lindiwe Khotseng [1,*]

[1] Department of Chemistry, Faculty of Natural Science, University of the Western Cape, Robert Sobukwe Road, Private Bag X17, Bellville 7535, South Africa; 4264957@myuwc.ac.za
[2] Council for Scientific and Industrial Research, Pretoria 0001, South Africa
* Correspondence: 3754640@myuwc.ac.za (N.S.S.); lkhotseng@uwc.ac.za (L.K.)

Abstract: In response to the increasing global demand for sustainable energy alternatives, this research explores the efficient conversion of sugarcane bagasse to bio-oil through hydrothermal liquefaction (HTL) processes with modified Zeolite Socony Mobil-5 catalysts (ZSM-5). The study systematically investigates the impact of feedstock quantity, reaction temperature, duration, and catalyst loading on bio-oil yield and quality. Optimisation experiments revealed that a feedstock amount of 10 grammes, an HTL temperature of 340 °C for 60 min and a ZSM-5 catalyst loading of 3 grammes resulted in the highest bio-oil yield. Furthermore, the introduction of Ni and Fe metals to ZSM-5 exhibited enhanced catalytic activity without compromising the structure of the zeolites. Comprehensive characterisation of modified catalysts using SEM-EDS, XRD, TGA, TEM, and FTIR provided insight into their structural and chemical properties. The successful incorporation of Ni and Fe into ZSM-5 was confirmed, highlighting promising applications in hydrothermal liquefaction. Gas chromatography–mass spectrometry (GC-MS) analysis of bio-oils demonstrated the effectiveness of the 2% Fe/ZSM-5 catalyst, highlighting a significant increase in hydrocarbon content. FTIR analysis of the produced bio-oils indicated a reduction in functional groups and intensified aromatic peaks, suggesting a shift in chemical composition favouring aromatic hydrocarbons. This study provides valuable information on HTL optimisation, catalyst modification, and bio-oil characterisation, advancing the understanding of sustainable biofuel production. The findings underscore the catalytic prowess of modified ZSM-5, particularly with iron incorporation, in promoting the formation of valuable hydrocarbons during hydrothermal liquefaction.

Keywords: sugarcane bagasse; ZSM-5; bio-oil; hydrothermal liquefaction

Citation: Jideani, T.; Seroka, N.S.; Khotseng, L. Production of Bio-Oil from Sugarcane Bagasse through Hydrothermal Liquefaction Processes with Modified Zeolite Socony Mobil-5 Catalyst. *Catalysts* **2024**, *14*, 631. https://doi.org/10.3390/catal14090631

Academic Editor: Christos Kordulis

Received: 12 July 2024
Revised: 14 September 2024
Accepted: 15 September 2024
Published: 18 September 2024

1. Introduction

As global demand for sustainable energy sources continues to increase, the exploration of renewable and environmentally friendly alternatives becomes imperative [1]. The depletion of fossil fuel resources and the growing concerns about environmental sustainability have intensified global interest in renewable and sustainable energy sources [2]. Among these, biofuels derived from biomass offer a promising alternative, using organic materials to produce fuels that are less carbon intensive and potentially more sustainable than traditional fossil fuels. Sugarcane bagasse, a byproduct of sugarcane processing, represents a significant biomass resource with potential for the production of biofuels through advanced conversion technologies [3]. In this context, lignocellulosic biomass, such as sugarcane bagasse, emerges as a promising feedstock for the production of biofuels due to its abundance, renewability, and economic viability [4].

In response to the increasing global demand for sustainable energy alternatives, this research explores the efficient conversion of sugarcane bagasse into bio-oil through hydrothermal liquefaction (HTL) processes with modified Zeolite Socony Mobil–5 (ZSM-5) catalysts.

Hydrothermal liquefaction (HTL) is a prominent method for transforming biomass into valuable bio-oil among the various conversion technologies. Hydrothermal liquefaction is a thermochemical process that converts biomass in a high-pressure, high-temperature aqueous environment, mimicking the natural processes of fossil fuel formation into liquid oil [5]. The process offers advantages over traditional pyrolysis or fermentation methods by allowing for higher conversion efficiencies and producing a higher quality bio-oil with fewer oxygenated compounds [6].

In the pursuit of enhancing the efficiency and selectivity of this conversion process, catalytic strategies have gained considerable attention. Zeolite Socony Mobil–5 (ZSM-5), renowned for its acidic sites and shape-selective characteristics, presents an intriguing catalyst for improving the yield and quality of bio-oil derived from sugarcane bagasse [7,8]. Catalysts can significantly influence the reaction kinetics, product distribution, and overall energy efficiency of the HTL process. Among the various catalysts studied, zeolite Socony Mobil-5 (ZSM-5), a type of microporous aluminosilicate material, has shown promise due to its acidity, shape selectivity, and stability under HTL conditions. Modified forms of ZSM-5 catalysts have been particularly explored for their ability to tailor bio-oil composition by promoting deoxygenation reactions and reducing the presence of oxygenates that can affect fuel properties [9].

Previous studies have demonstrated the importance of optimising catalyst loading to maximise bio-oil yield and quality [10]. For example, varying the amount of ZSM-5 can influence the reaction kinetics and the distribution of the bio-oil components, affecting both the energy content and the stability of the resulting biofuel [11]. Furthermore, the amount of feedstock used in the reaction also plays a crucial role in determining the overall efficiency of the HTL process, as excessive feedstock may lead to unfavourable conditions, including limitations in mass transfer and increased char formation [12].

This research aims to investigate the optimal conditions for producing bio-oil from sugarcane bagasse using a modified Zeolite Socony Mobil-5 catalyst, focusing on the effects of varying catalyst loading, the duration of the reaction, and feedstock quantities. By elucidating the relationships between these factors and the resulting bio-oil characteristics, this research seeks to contribute to the development of more efficient biomass conversion processes, ultimately supporting the transition toward renewable energy sources.

The results of this investigation have the potential to advance the bioenergy field, offering a scalable and environmentally sound approach to converting sugarcane bagasse into a valuable liquid fuel resource. As the world seeks innovative solutions to mitigate the impact of traditional fossil fuels, this study is at the intersection of biomass use and catalytic technology, paving the way for a more sustainable and economically viable bio-oil production process.

2. Results and Discussion

The hydrothermal liquefaction of sugarcane bagasse produced a variety of valuable products, primarily bio-oil, which is a complex mixture of organic compounds including phenols, aldehydes, ketones, and hydrocarbons. This bio-oil can be further refined into fuels or chemicals. Alongside bio-oil, HTL also generated an aqueous phase rich in water-soluble organic compounds. Additionally, a solid residue called biochar was produced, consisting mostly of carbon and inorganic minerals, which can be utilized as a soil amendment or activated carbon. The process also yielded a gaseous phase composed mainly of carbon dioxide and minor amounts of methane, hydrogen, and other light hydrocarbons. These products collectively highlight the potential of HTL to convert biomass into a range of valuable materials and energy sources.

2.1. XRD

X-ray diffraction (XRD) is a pivotal analytical technique for elucidating the atomic and molecular arrangement of crystalline materials. The samples were analysed using a Rigaku MiniFlex 600 X-ray Diffractometer.

Observed in Figure 1, the results of the XRD experiment reveal crucial information about ZSM-5 and metal-doped ZSM-5 catalysts. In particular, the sharp and intense peaks observed suggest that the crystallinity of ZSM-5 remained unaffected after the wet impregnation of metals on it. The XRD pattern of the ZSM-5 catalyst exhibits the characteristic MFI peaks, notably around 8–10°, 22–23° 2θ, and 29.91° matched well with the ZSM-5 planes (JCPDS cards) No. 00-047-0638) [13]. The absence of observable metal incorporation in the ZSM-5 and ZSM-5 metal-doped XRD patterns may be attributed to the fact that metal ions introduced during doping are dispersed on the surface or within the pores of the ZSM-5 framework rather than being integrated into the crystal lattice. This phenomenon is common when metal ions are introduced through methods such as impregnation, where the metal species tend to form small, highly dispersed clusters or isolated atoms on the zeolite surface, which may be below the detection limit of XRD [14,15].

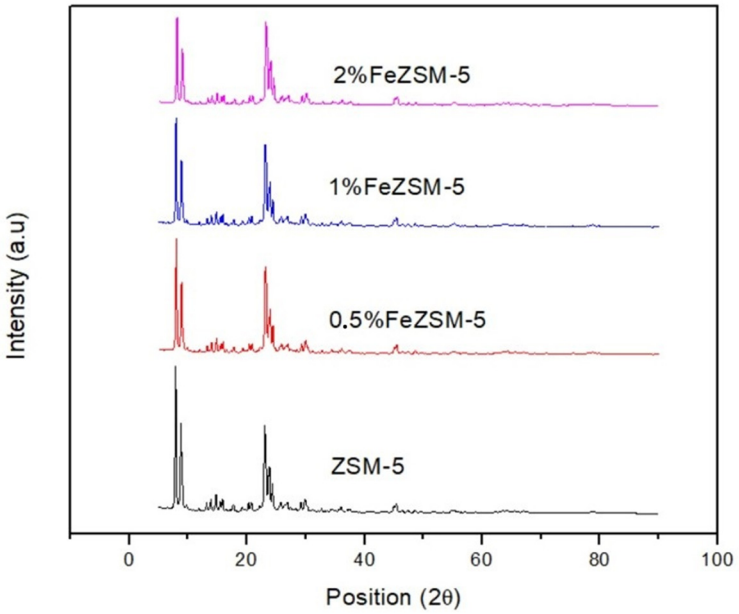

Figure 1. XRD spectra showing ZSM-5 and Fe-doped ZSM-5.

Figure 1 shows the XRD patterns of the ZSM-5 zeolite catalyst modified with iron (Fe). There is no discernible alteration in the primary crystal structure of the ZSM-5 catalyst. The absence of characteristic peaks associated with iron in the spectra indicates that iron was effectively distributed throughout the ZSM-5 zeolite catalyst without forming large crystalline structures. This observation aligns with the findings from the catalyst's EDS analysis.

2.2. FTIR

The seven catalysts samples are ZSM-5, 0.5% NiZSM-5, 0.5% FeZSM-5, 1% NiZSM-5, 1% FeZSM-5, 2% NiZSM-5 and 2% FeZSM-5. All the ZSM-5 catalysts were analysed using an FTIR Perkin Elmer spectrophotometer.

The infrared spectrum shown above shows Figures 2 and 3 and specific peaks can be observed in different regions, providing valuable information on the molecular structure of the analysed sample. In the 3500–3800 cm^{-1} range, the peaks are explained as stretching vibrations of hydrogen linked to Si-OH groups, suggesting the existence of hydroxyl groups (OH) in the samples. These groups are commonly found in compounds such as alcohols, phenols, and carboxylic acids. Another significant peak, observed around 2900 cm^{-1}, is associated with C-H stretching vibrations, indicating the presence of carbon-hydrogen bonds in the sample. This peak is typical for various organic compounds, including alkanes, alkenes, and alkynes. The presence of C-H bonds detected by FTIR in ZSM-5 zeolite catalysts can be attributed to hydrocarbon residues, which may originate from the

synthesis of ZSM-5. During synthesis, organic molecules, such as solvents, can become trapped within the zeolite pores, and these organic species often contain C-H bonds that are detectable by FTIR. Furthermore, ZSM-5 zeolites possess surface hydroxyl groups that function as Brnsted acid sites. These hydroxyl groups can interact with adsorbed hydrocarbons, trace amounts of water, or alcohols, leading to the formation of C-H bonds on the surface [16].

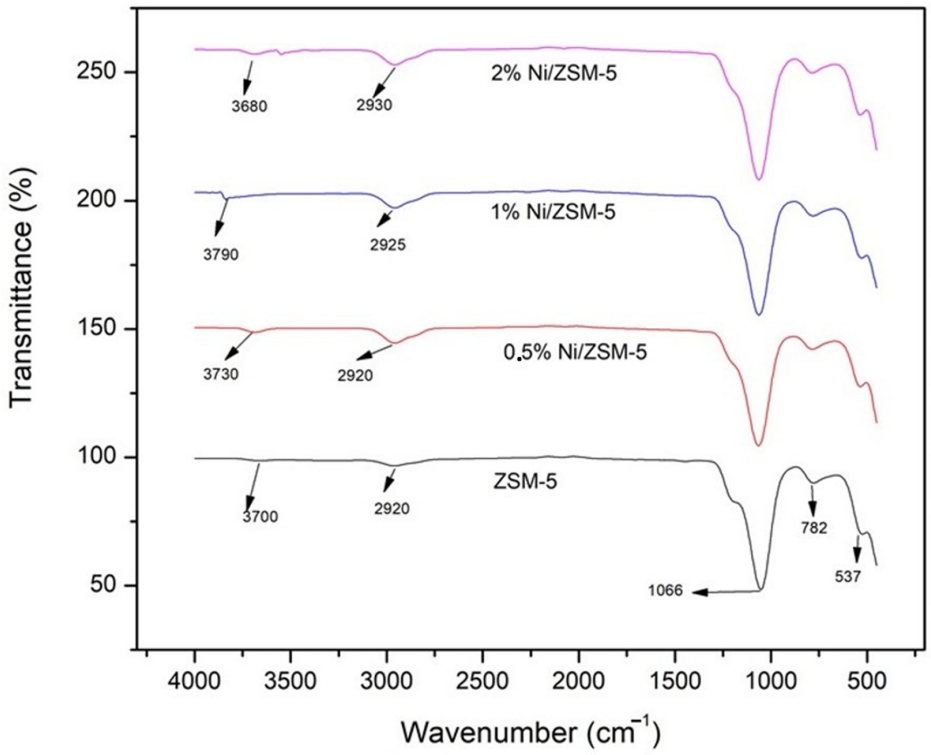

Figure 2. FTIR spectrum showing the different nickel-modified ZSM-5 catalysts.

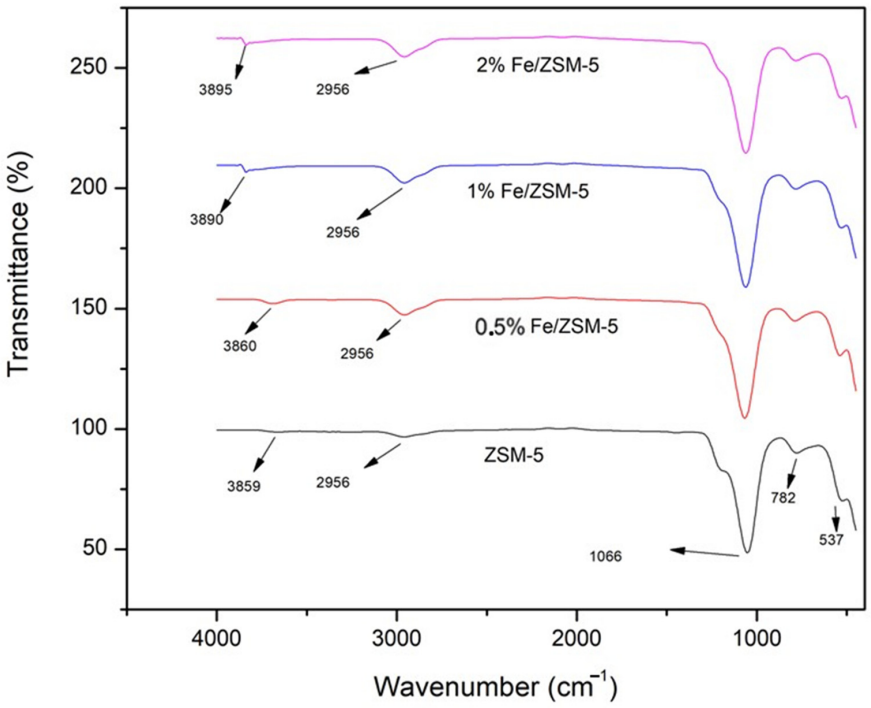

Figure 3. FTIR spectrum showing the different iron-modified ZSM-5 catalysts.

Furthermore, peaks are observed around 1066 cm^{-1}, which can be attributed to Si-O stretching vibrations, indicating the presence of Si-O bonds. These bonds are characteristic of various silicates and siloxane compounds. Furthermore, another peak is observed around 537 cm^{-1}, and in both spectra, this can be attributed to the five-membered ring of the pentasil zeolite structure [17]. The peak at 782 cm^{-1} is attributed to the presence of Ni-O and Fe-O on the catalytic surface. These results are in agreement with the work by Sarve et al. [18]. In both instances where ZSM-5 was modified with nickel or iron, the spectra depicted in Figures 3 and 4 reveal a slight elevation in the intensity of the band associated with OH groups coordinated to extra-framework T-atoms. This suggests a migration of the metals to the extra framework sites in the ZSM-5 catalysts impregnated with nickel or iron. In particular, there is no evidence of isomorphous substitution within the ZSM-5 framework after modifications with Ni and Fe, as indicated by the absence of significant shifts in the positions of the bands [19].

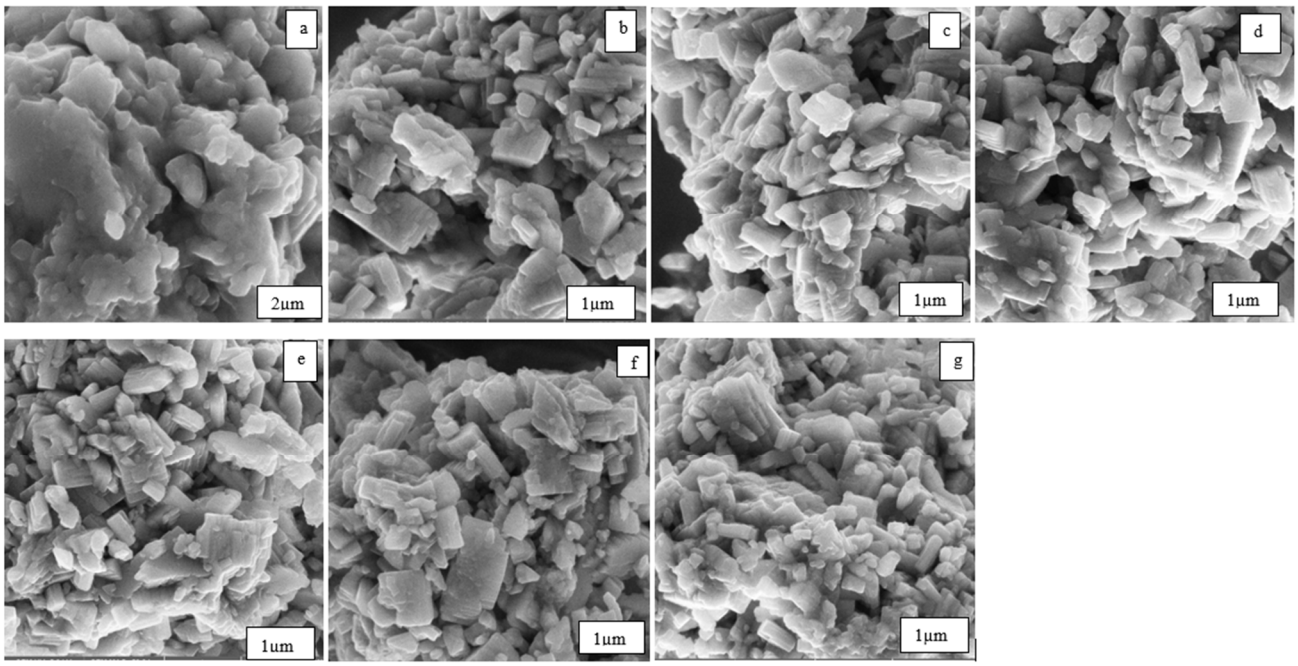

Figure 4. SEM micrographs (**a**) ZSM-5, (**b**) 0.5% Fe/ZSM-5, (**c**) 0.5% Ni/ZSM-5, (**d**) 1% Fe/ZSM-5, (**e**) 1% Ni/ZSM-5, (**f**) 2% Fe/ZSM-5, and (**g**) 2% Ni/ZSM-5.

2.3. SEM-EDS

SEM provides detailed surface morphology and microstructural information, while EDS enables the identification and quantification of elements present in the sample. The SEM images were examined at an accelerating voltage of 2 kV using a TESCAN Vega TC instrument equipped with an X-ray detector for energy-dispersive X-ray analysis (EDS) operating at 5 kV.

The morphology of ZSM-5 and modified ZSM-5 was evaluated using SEM. Figure 4 shows the SEM micrographs of these materials. Interestingly, there is no noticeable difference in the morphology of ZSM-5 crystals before and after metal doping, as evident from the SEM micrographs. The larger spherical structures appear to be aggregates of smaller crystals. In Figure 4a, the agglomerated crystals are shown, which exhibit a distinctive shape that resembles a slightly hexagonal structure, which is recognised as a characteristic form of ZSM-5 [20]. Interestingly, the morphology of ZSM-5 doped with metals closely resembles that of ZSM-5; this is in agreement with previous research done by Sarve et al. [18]. These findings strongly suggest that the fundamental structure of the MFI zeolite remains unchanged even with the introduction of metals, Figure 5a–d. The Fe/Ni-ZSM-5 catalysts maintain the characteristic cubic morphology of ZSM-5 zeolites. Additionally, small crys-

talline particles observed on the surface of the ZSM-5 catalysts are likely attributed to the presence of Fe/Ni species dispersed on the external surface of the Fe/Ni-ZSM-5 catalysts. This surface distribution of metal species is consistent with similar observations reported in the literature, where metal dopants tend to form small, highly dispersed clusters on the zeolite surface rather than integrating into the crystal lattice [21].

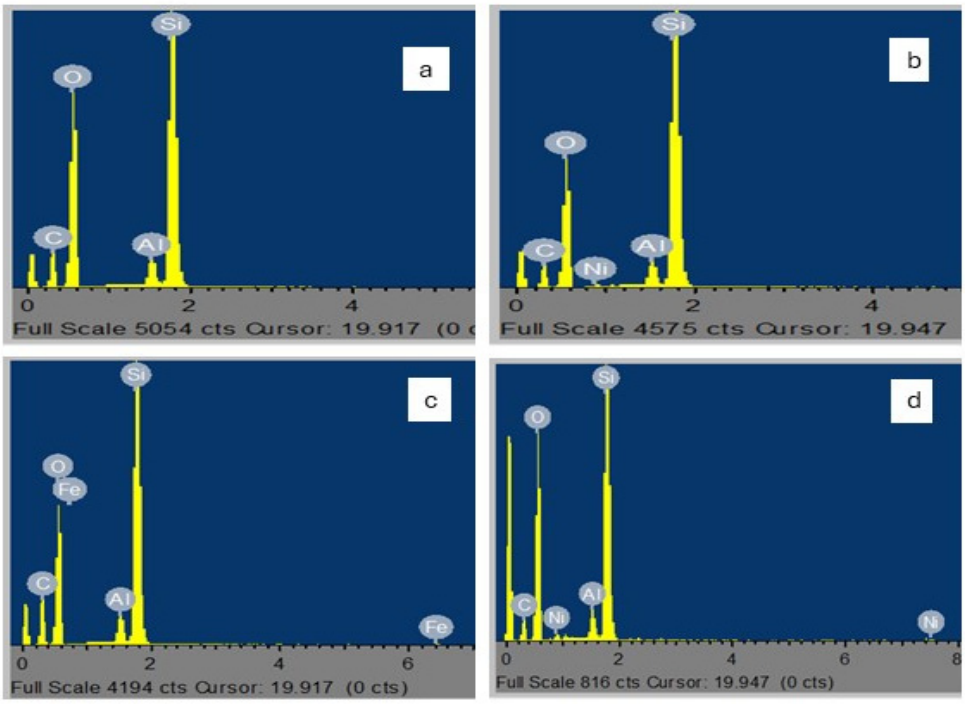

Figure 5. EDS results of metal-doped ZSM-5. (**a**) 0.5% Fe/ZSM-5, (**b**) 0.5% Ni/ZSM-5, (**c**) 1% Fe/ZSM-5, (**d**) 1% Ni/ZSM-5.

The results of the elemental analysis, depicted in Figure 6, relate to ZSM-5 and modified ZSM-5. These findings reveal the presence of Ni and Fe after wet impregnation of ZSM-5. Specifically, 2% FeZSM-5 showed an average Fe content of approximately 0.33% on ZSM-5, while 2% Ni showed an average Ni content of around 0.73% on ZSM-5. These results provide compelling evidence of the even distribution of these metals on the surface of ZSM-5. Importantly, these metal loadings do not significantly alter the fundamental structure of ZSM-5, confirming its structural integrity. Figure 6 above shows the EDS results for 0.5% Fe/ZSM-5, 0.5% Ni/ZSM-5, 1% Fe/ZSM-5, and 1% Ni/ZSM-5, these results show the presence of metals on the surface of the catalysts. Detailed relative compositions are tabulated in Table 1 below.

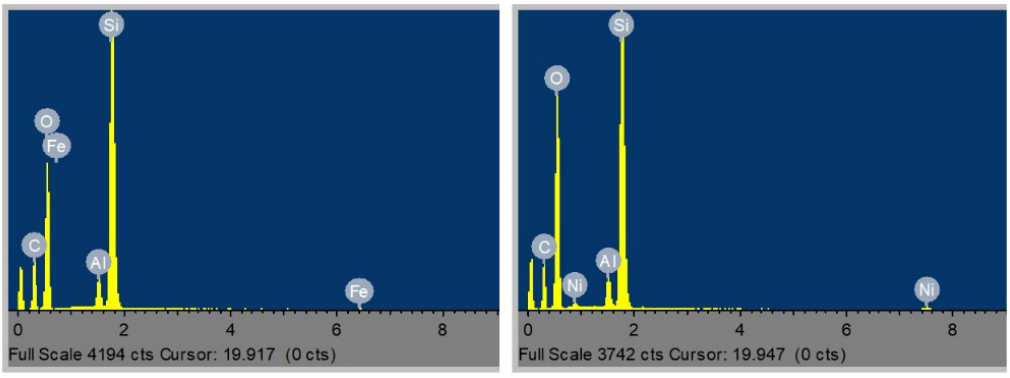

Figure 6. EDS results for 2% Fe/ZSM-5 and 2% Ni/ZSM-5 catalysts.

Table 1. EDS results for all catalysts, ZSM-5, and Fe- and Ni-modified ZSM-5.

Catalyst	Elements					
	C (Atomic %)	O (Atomic%)	Al (Atomic %)	Si (Atomic %)	Fe (Atomic %)	Ni (Atomic%)
ZSM-5	31.36	47.47	1.58	19.58	-	-
0.5% Fe/ZSM-5	27.06	57.86	1.6	19.43	0.04	-
0.5% Ni/ZSM-5	21.61	54.07	1.78	22.44	-	0.11
1% Fe/ZSM-5	35.86	47.13	1.33	15.54	0.14	-
1% Ni/ZSM-5	21.62	54.59	1.84	21.58	-	0.37
2% Fe/ZSM-5	21.82	53.17	1.86	22.82	0.33	-
2% Ni/ZSM-5	23.01	53.68	1.71	20.87	-	0.73

2.4. TGA

The thermal stability and behaviour of the samples were investigated using the thermogravimetric analysis (TGA) technique with a PerkinElmer Simultaneous Thermal Analyzer (STA 8000). The TGA analysis was performed from room temperature (30 °C) to 800 °C at a heating rate of 10 °C/min, followed by cooling at 40 °C/min. This was carried out in the seven samples, which are ZSM-5, 0.5% NiZSM-5, 0.5% FeZSM-5, 1% NiZSM-5, 1% FeZSM-5, 2% NiZSM-5, and 2% FeZSM-5.

From Figure 7, the TGA results show the thermal behaviour and weight loss patterns of seven samples: ZSM-5, 0.5% NiZSM-5, 0.5% FeZSM-5, 1% NiZSM-5, 1% FeZSM-5, 2% NiZSM-5, and 2% FeZSM-5. The temperature range of the analysis is from 0 to 800 °C. Based on the provided TGA results, it can be observed that the samples show weight loss at elevated temperatures. From 50 to 240 °C, all samples experience approximately 4% to 8% weight loss. Similar results can be seen in the work by Pengfei et al. (2021) [22]. Subsequently, in the temperature range of 250 to 800 °C, another 8% weight loss is observed. Beyond 800 °C, no additional weight loss is recorded. The significant mass loss observed in the TGA data for ZSM-5, Fe/ZSM-5, and Ni/ZSM-5 is probably related to the desorption and decomposition of various components present within the zeolite structure. Initially, the mass loss could be attributed to the removal of physically adsorbed water and moisture from the zeolite pores, which typically occurs at lower temperatures. As the temperature increases, a more substantial mass loss may be observed, corresponding to the decomposition of organic species, such as residual structure-directing agents or organic solvents used during the synthesis of the zeolites. These organics are often trapped within the zeolite framework and are gradually released upon heating [23].

For the metal-doped samples (Fe/ZSM-5 and Ni/ZSM-5), the mass loss could also be associated with the reduction and oxidation processes of the metal species, as well as the decomposition of any metal-organic complexes or surface-bound species formed during the doping process [24]. Although some weight loss is observed, the absence of further weight loss beyond 800 °C suggests that the samples may have reached a relatively stable state at higher temperatures.

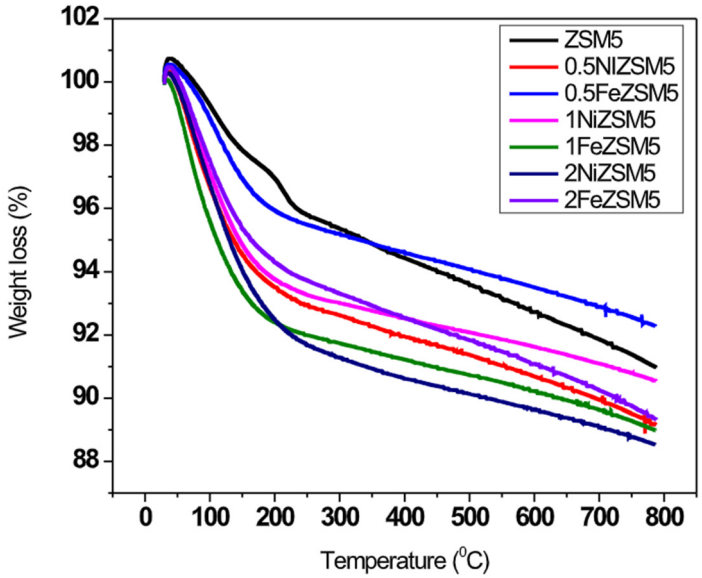

Figure 7. TGA curve for all ZSM-5 catalysts. ZSM-5, 0.5% Fe/ZSM-5, 0.5% Ni/ZSM-5, 1% Fe/ZSM-5, 1% Ni/ZSM-5, 2% Fe/ZSM-5, and 2% Ni/ZSM-5.

2.5. TEM

Structural analysis of the prepared catalysts was conducted using transmission electron microscopy (TEM), specifically using the JEOL 2100 model, as shown in Figure 8 below.

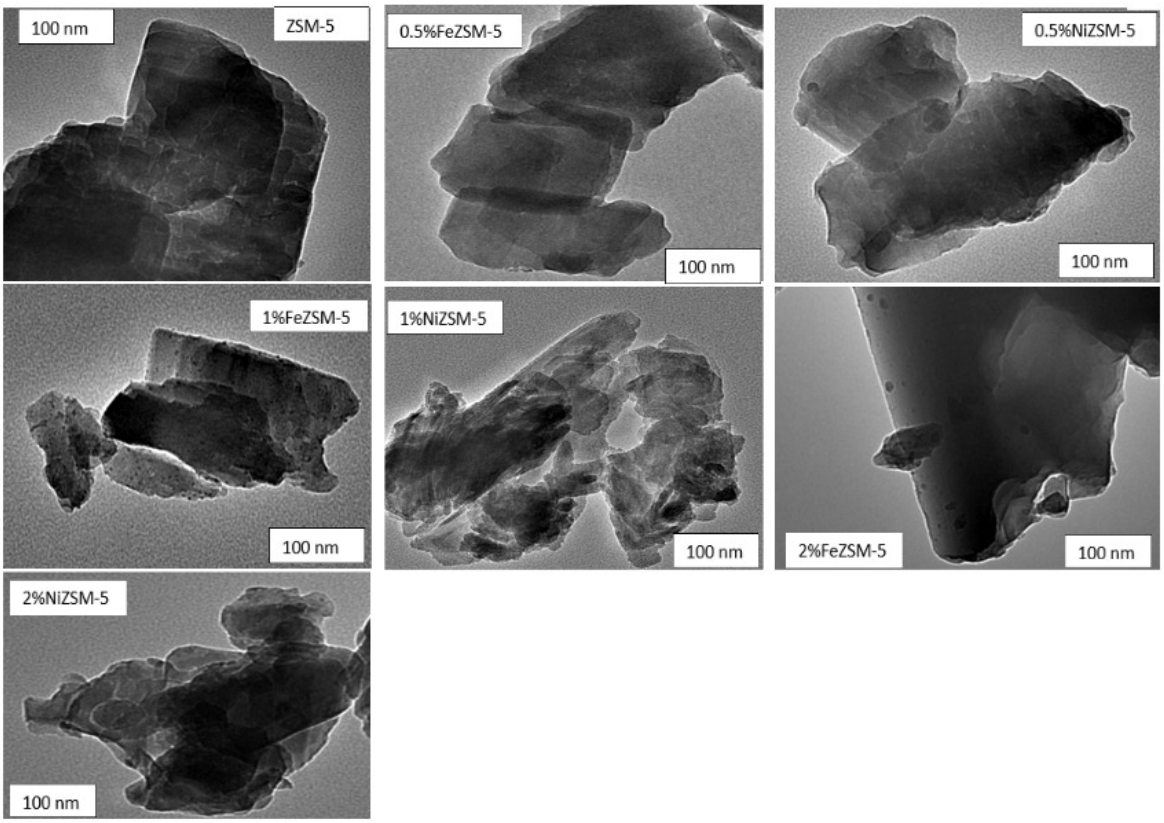

Figure 8. TEM images for all ZSM-5 catalysts.

The TEM images, as shown in Figure 8 of the modified ZSM-5 zeolite sample, reveal nanocrystals with distinct bright areas, indicating the existence of mesopores. Dark regions

dispersed among the bright contrast appear as bright contrast in the bright-field image. This mode of mass-thickness sensitive suggests the successful doping of mesoporous ZSM-5, where mesopores coexist with the three-dimensional microporosity of the zeolite framework [25].

The TEM images of pure ZSM-5 exhibit well-defined cubic or coffin-shaped crystals, with visible lattice fringes and an interconnected network of micropores, reflecting its highly ordered, porous framework [26]. For Fe/ZSM-5 and Ni/ZSM-5, the TEM images show the ZSM-5 crystals decorated with small, dark spots or clusters corresponding to Fe and Ni nanoparticles, respectively. These metal species are typically dispersed on the surface or within the pores of zeolite, their distribution and size varying depending on the synthesis method and the metal load [27]. Importantly, the cubic morphology of ZSM-5 was retained in both metal-doped samples, indicating that the doping process has not significantly altered the overall zeolite structure. The observed dispersion and size of the metal particles provide information on the effectiveness of doping and the potential catalytic properties of modified zeolites [28].

3. Materials and Experimental Method

3.1. Materials Used

All chemicals in this research were obtained from KIMIX Chemical & Lab Supplies cc Cape Town and used without further purification. Nickel nitrate, iron nitrate, and dichloromethane were purchased from KIMIX and used without further purification. All synthesis was performed using deionised water from the Milli-Q water purification system) with a conductivity of 32.6 uScm^{-1}. (Millipore, Bedford, MA, USA). Sugarcane bagasse, sourced from Illovo Sugar Ltd. in Durban, South Africa, was the feedstock chosen for this research. The bagasse was washed and allowed to air-dry for 24 h. Once dried, it was ground with a mortar and pestle until the particles were approximately 2.0 mm in size. The selection of sugarcane bagasse was based on its abundant availability as an agricultural by-product. Often considered waste and an environmental pollutant, readily accessible biomass offered a promising and sustainable option for biofuel production.

3.2. Catalyst Preparation

The ZSM-5 catalyst used in this study was previously synthesized and characterized by its specific surface properties. It exhibited a BET surface area of 328 m^2/g, which indicates the total surface area available for adsorption. The micropore area, accounting for 240 m^2/g, reflects the surface area within the zeolite's microporous structure, highlighting its capability to adsorb small molecules. Additionally, the catalyst had a pore volume of 0.069 cm^3/g, representing the volume of pores available for adsorption and diffusion of reactants and products. These properties make ZSM-5 a highly suitable catalyst for various catalytic applications, especially in reactions involving hydrocarbon transformations.

To obtain pure H-ZSM-5, NH_4-ZSM-5 was subjected to a conversion process by calcination at 500 °C for 5 h. Metal-doped ZSM-5 catalysts were prepared using the incipient wetness impregnation method [29]. Initially, a small amount of water was used to suspend the zeolite powder in one beaker, while in another beaker, the M-metal salt (nickel or iron) was dissolved and added dropwise to the zeolite powder in the solution. The mixture was stirred and heated to remove excess water and then dried in an oven at 100 °C for an hour. Subsequently, the resulting product was calcined at 550 °C for 5 h to obtain the ZSM-5 catalysts doped with metals. In Figure 9, a 2% Fe ZSM-5 catalyst is depicted, carefully weighed, and ready for use in the catalytic hydrothermal process. This image captures the precise amount of catalyst required for the experiment, ensuring precision and reproducibility in the subsequent steps of the hydrothermal liquefaction.

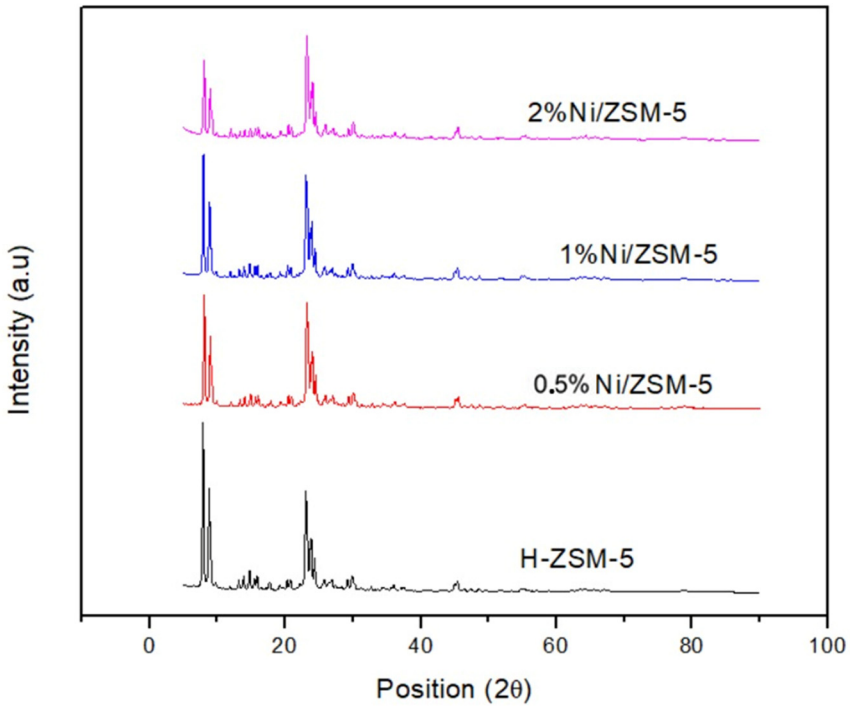

Figure 9. XRD spectra showing ZSM-5 and Ni-doped ZSM-5.

Catalysts with metal loadings of 0.5 wt%, 1 wt%, and 2 wt% were prepared, denoted as 0.5%Ni/ZSM-5, 1%Ni/ZSM-5, 2%Ni/ZSM-5, 0.5%Fe/ZSM-5, 1%Fe/ZSM-5, and 2%Fe/ZSM-5. To prepare 5 g of metal-modified ZSM-5 catalysts, 4.95 g of pristine ZSM-5 were mixed with 0.05 g of the respective metal (nickel or iron). The amount of metal to be added was calculated based on the desired percentage of metal loading. For example, in the case of nickel, 1% of 5 g (total mass of the catalyst) is 0.05 g of nickel.

The same calculations were made for the rest of the nickel and iron metals. Once all of the catalysts were prepared, they were stored in a desiccator for future use. The same method was employed to produce additional batches of the catalysts.

3.3. Production of Bio-Oil

3.3.1. Hydrothermal Liquefaction Process

Hydrothermal liquefaction was conducted using water as a solvent, with 200 mL of deionised water consistently used in all experiments. A suspension was prepared by mixing sugarcane bagasse with 200 mL of deionised water, which was then loaded into a 1 L autoclave. For experiments involving a catalyst, it was added to the slurry. The autoclave was placed in the hydrothermal liquefaction system and gradually heated from room temperature to 340 °C at a controlled rate of 10 °C per minute. After the designated reaction time, the autoclave was cooled to room temperature and its contents were transferred to a beaker and filtered using vacuum filtration. The resulting filtrate was moved to a separation funnel, where dichloromethane (DCM) was added for liquid–liquid extraction. DCM selectively extracted organic compounds, including bio-oil, from the aqueous phase. The organic layer containing bio-oil was collected in a round-bottom flask, which underwent rotary evaporation to remove the DCM solvent, leaving behind the bio-oil residue. The final step involved weighing the collected bio-oil to determine its yield. The solid residue collected on filter paper was carefully collected and dried overnight in an oven at 100 °C to remove any remaining moisture for precise measurement.

3.3.2. The Effect of Temperature on the Reaction

The yield obtained at 340 °C was 3.016 wt%. Research indicates that raising the process temperature positively impacts both bio-oil production and the higher heating value (HHV),

as demonstrated by various studies [30]. Tshimangadzo et al. further established that temperatures below 300 °C can result in incomplete conversion, generating solid biochar and gaseous by-products with associated losses. On the contrary, temperatures exceeding 340 °C tend to favour the formation of gaseous products [31]. Javier A. et al. also determined that 340 °C is suitable for optimal bio-oil yield [3]. This illustrates the significant impact of temperature on the biomass conversion process. Elevated temperatures improve the thermal decomposition of biomass, leading to accelerated reaction rates and promoting the effective depolymerisation of complex carbohydrates and lignin into smaller molecular fragments [32]. While higher temperatures can initially increase bio-oil yields, they may also result in char or gaseous by-products, underscoring the importance of identifying an optimal temperature range that maximises the yield of liquid products while minimising the formation of solid residues [33]. Moreover, the composition of the bio-oil produced can vary with temperature, significantly influencing its quality and stability. Operating at elevated temperatures may require increased energy input, which could affect the overall economic viability of the HTL process. Therefore, balancing yield, product quality, and operational costs is crucial to successfully converting sugarcane bagasse into biofuels.

3.3.3. The Effect of Residence Time

It was determined by previous studies that it takes 30 min for the reactor to reach the desired temperature [3]. Based on the research conducted by Tshimangadzo et al. in 2022, it was determined that hydrothermal liquefaction (HTL) carried out at a temperature of 340 °C for a duration of 60 min resulted in the optimal bio-oil yield. Therefore, considering this result, the 60 min duration was adopted as the optimal condition for the hydrothermal liquefaction process. This finding suggests that at 340 °C for 60 min, the conditions were conducive to maximising bio-oil production from the given feedstock [7]. The experiment was carried out for 60 min at 340 °C. The measured bio-oil yield under these conditions was found to be 3.016 by weight. The observed bio-oil yield of 3.016 by weight at 60 min indicates that this specific duration and temperature combination efficiently break down complex organic compounds in the sugarcane bagasse feedstock. The 60 min duration allows sufficient time for the thermal cracking and decomposition reactions to occur, producing a considerable quantity of bio-oil. Optimising the duration is crucial to achieving the highest possible bio-oil yield, while ensuring an economically viable and energy-efficient process.

3.3.4. The Effect of the Ratio of Feedstock to Catalyst

The influence of the catalyst-to-feedstock ratio on bio-oil production was systematically investigated using different loadings of pure ZSM-5 catalyst at 20%, 30% and 50%. The corresponding bio-oil yields were 3.793 wt%, 4.647 wt%, and 2.363 wt%, respectively. These results indicate that increasing catalyst loading initially enhances catalytic efficiency, as evidenced by the higher bio-oil yield at 30% ZSM-5. However, further increasing the catalyst loading to 50% led to a decline in bio-oil yield.

Among the catalyst loadings tested, 30% ZSM-5 achieved the highest bio-oil yield, suggesting an optimal catalytic effect at this ratio. The bio-oil yield of 4.647 by weight obtained with 30% ZSM-5 demonstrates a more efficient promotion of hydrothermal liquefaction (HTL) reactions compared to the other loadings. This catalyst loading balances catalytic activity and bio-oil production, while also considering process efficiency and cost-effectiveness.

When these findings are compared with those of the literature, the observed trend is consistent with studies that highlight the critical role of catalyst loading in HTL processes. For instance, previous research by Reza et al. demonstrated that moderate catalyst loadings often yield higher bio-oil outputs, while excessive loadings can lead to secondary reactions that diminish overall yield. Similarly, Singh et al. reported that optimal catalyst loadings are crucial for balancing reaction kinetics and minimising undesirable by-products. The

selection of 30% ZSM-5 aligns well with these studies, reinforcing its efficacy in enhancing bio-oil production through HTL.

4. Product Analysis: Bio-Oil

4.1. Bio-Oil Yield

The impact of modified ZSM-5 catalysts on biomass conversion was assessed using various catalysts. ZSM-5, 0.5% Fe/ZSM-5, 0.5% Ni/ZSM-5, 1% Fe/ZSM-5, 1% Ni/ZSM-5, 2% Fe/ZSM-5, and 2% Ni/ZSM-5 for the conversion of sugarcane bagasse to bio-oil.

The results revealed that the 2% Fe/ZSM-5 catalyst produced the highest bio-oil yield at 8.09%, equivalent to 0.81 g in mass, followed by 2% Ni/ZSM-5, 1% Fe/ZSM-5, 0.5% Fe/ZSM-5, 1% Ni/ZSM-5, 0.5% Ni/ZSM-5, and ZSM-5, with yields of 6.86%, 6.71%, 5.52%, 5.10%, 3.98%, and 2.99%, respectively, as shown in Figure 10 above. This indicates that the modified 2% Fe/ZSM-5 catalyst effectively facilitated the conversion of various components into bio-oil constituents. The results underscore the promotion of the hydrothermal process with modified ZSM-5 catalysts, leading to improved bio-oil yields. Furthermore, the stability of these catalysts significantly enhanced the hydrothermal conversion of sugarcane bagasse, with the use of 2% Fe/ZSM-5 resulting in more than double the bio-oil mass compared to ZSM-5 alone, producing 0.81 g of bio-oil compared to 0.30 g with ZSM-5 alone.

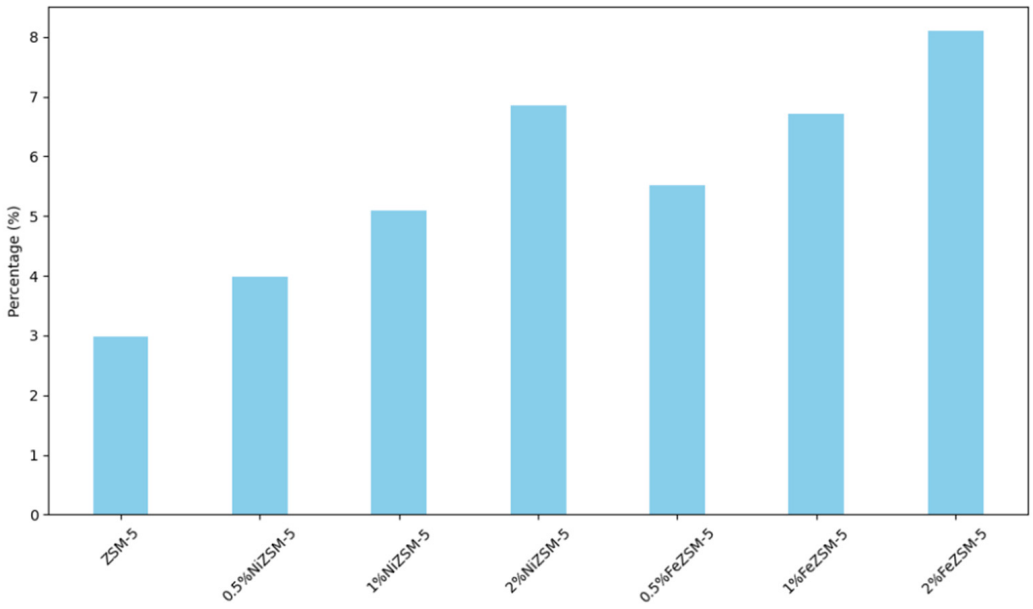

Figure 10. A bar graph showing the effect of catalyst on the bio-oil yield.

4.2. GC-MS

GC-MS analysis identified numerous volatile chemical compounds, which were categorised into different classes. Oxygenated compounds, including ketones, alcohol, ethers, esters, and aldehydes. Organic acids, including fatty acids, carboxylic acids, and fatty acids methyl esters. Cyclic oxygenate, including furans and pyrans. Aromatics, including phenols, phenyls, and arenes. Nitrogenated compounds, including azides, amines, amides, nitriles, imines, and azoles. Hydrocarbons, including straight chains of alkanes, alkenes, and alkynes. The column oven was initially kept at a temperature of 100 °C, while the auto-injector port temperature was kept at 250 °C. 1 µL of sample extract residues were then injected in split-less mode. Helium was used as the carrier gas with a flow rate of 1.0 mL/min and a pressure of 61.5 kPa. The temperature was first maintained at 100 °C for 2 min, increased at a rate of 15 °C/min to 180 °C (kept for 3 min), ramped at a rate of 5 °C/min to 250 °C for 3 min, and finally ramped at a rate of 20 °C/min to 320 °C and total run time was 40 min.

GC-MS analysis of bio-oil derived from hydrothermal liquefaction (HTL) of sugarcane bagasse was performed, as shown in Figure 11, revealing several chemical components. These components included nitrogenated compounds, cyclic oxygenates, aromatic compounds, organic acids, other miscellaneous compounds, and hydrocarbons. In particular, the bio-oil produced using the ZSM-5 catalyst exhibited a 48% content of oxygenated compounds, while the oil of 2% NiZSM-5 contained 37% of these compounds, and 2% Ni-loaded ZSM-5 produced 47% (see Figure 12). Furthermore, in Figure 12, it can be observed that there was an increase in the hydrocarbon content, from 7% for ZSM-5 to 8.6% for 2% FeZSM-5 and finally to 11.6% for 2% NiZSM-5, corresponding to higher metal loadings.

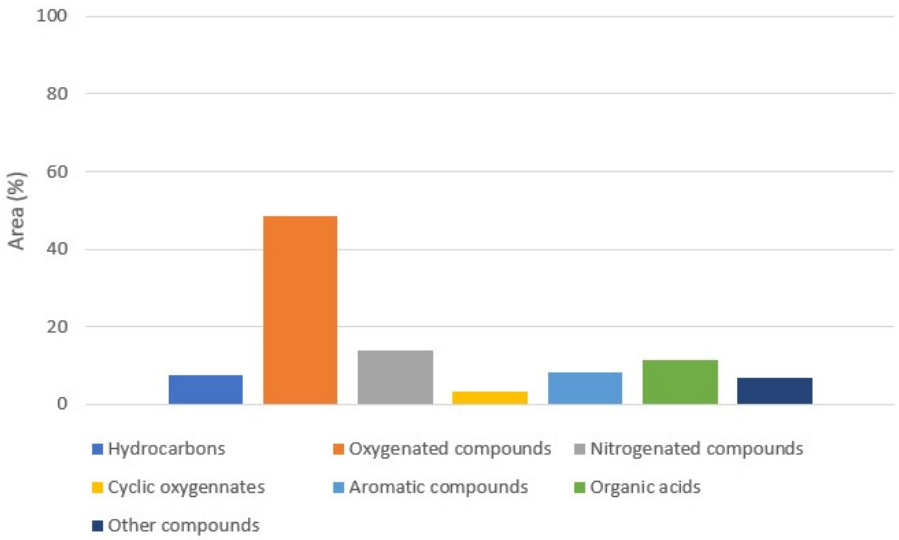

Figure 11. Main compounds analysed by GC-MS for the bio-oil obtained from HTL using ZSM-5.

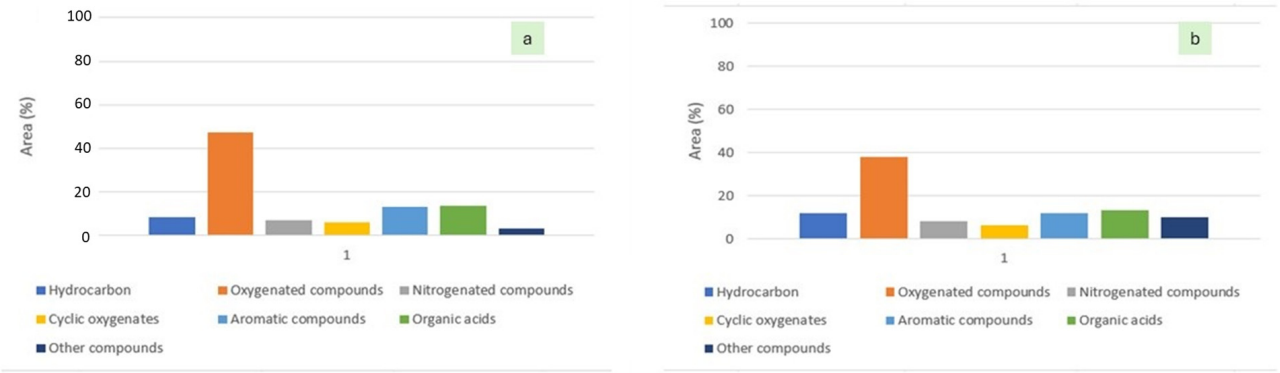

Figure 12. (**a**) Bio-oil obtained from 2% Fe/ZSM-5, (**b**) bio-oil obtained from 2% Ni/ZSM-5, analysed by GC-MS.

Figure 13 shows that 0.5% Fe/ZSM-5 had 38% oxygenated compounds, while hydrocarbons were 11.1% compared to 0.5% Ni/ZSM-5, which had 51% oxygenated compounds and 9% hydrocarbons. When comparing 1% Fe/ZSM-5, oxygenated compounds had 52%, hydrocarbons had 4%, and 1% Ni/ZSM-5 had 38% oxygenated compounds and 5% hydrogenated compounds.

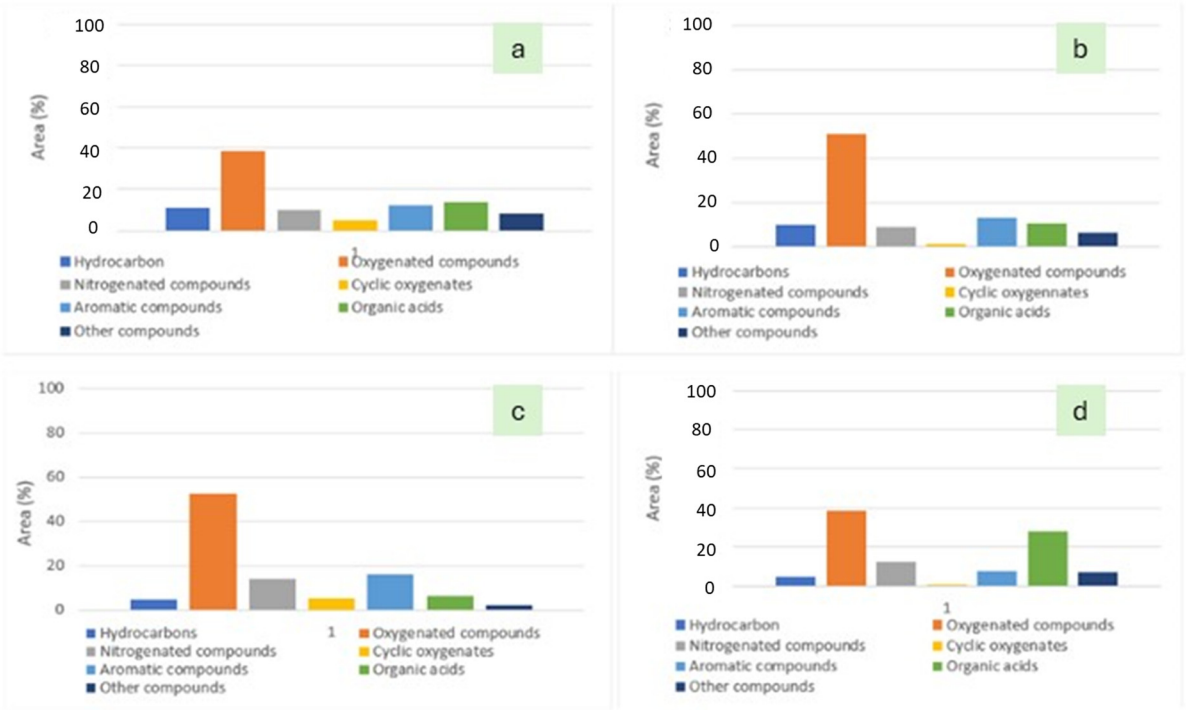

Figure 13. Main compounds analysed by GC-MS for the bio-oil obtained from HTL using (**a**) 0.5% Fe/ZSM-5, (**b**) 0.5% Ni/ZSM-5, (**c**) 1% Fe/ZSM-5, and (**d**) 1% Ni/ZSM-5.

The observed trend, shown in Figure 12a,b, indicates a notable increase in the hydrocarbon content of bio-oil when modified ZSM-5 catalysts are used compared to pure ZSM-5. In particular, the 2% Ni/ZSM-5 catalyst exhibited the lowest content of oxygenated compounds, Figure 12b. This phenomenon can be attributed to the presence of the modified ZSM-5 zeolite catalyst. Many of the oxygenated compounds probably reached the active sites located on the surface and within the channels of the zeolite catalyst. Consequently, this interaction led to a sequence of complex reactions, including cracking, dehydration, decarbonylation, decarboxylation, and oligomerization as well as subsequent processes, such as combination, aromatization, and cyclisation reactions, ultimately resulting in the generation of hydrocarbons.

4.3. FTIR

FTIR analysis was conducted on the bio-oils to assess the composition of functional groups. FTIR analysis was conducted using a Perkin Elmer FTIR spectrophotometer. The samples were carefully analysed within the 400 to 4000 cm^{-1} wavelength range. Before each sample measurement, background air spectra were collected. The samples were directly compressed onto attenuated total reflectance (ATR) crystals without any prior preparation. The diamond ATR crystal was cleaned using ethanol and distilled water prior to analysis. In the FTIR spectra of the bio-oils shown in Figure 14, several fundamental bands were identified at specific vibrational frequencies, including approximately 3291, 2905, 1565, 1372, 1031, and 879 cm^{-1}. A broad and intense absorption peak within the 3000–3600 cm^{-1} range was associated with OH or NH stretching vibrations, indicative of the presence of alcohols, phenols and heterocyclic compounds containing N. Furthermore, a peak spanning 2700 to 2900 cm^{-1} was associated with C-H stretching vibrations, attributed to the methyl and methylene groups in aliphatic and alkane compounds. Within the range of 1500 to 1750 cm^{-1}, peaks corresponding to C=O stretching bands were observed, signifying the presence of carboxylic acids, amides, ketones, and esters. Furthermore, a noticeable vibration between 1250 and 1500 cm^{-1} was assigned to the C=C band, indicating the existence of aromatic rings, particularly furan rings, in bio-oils.

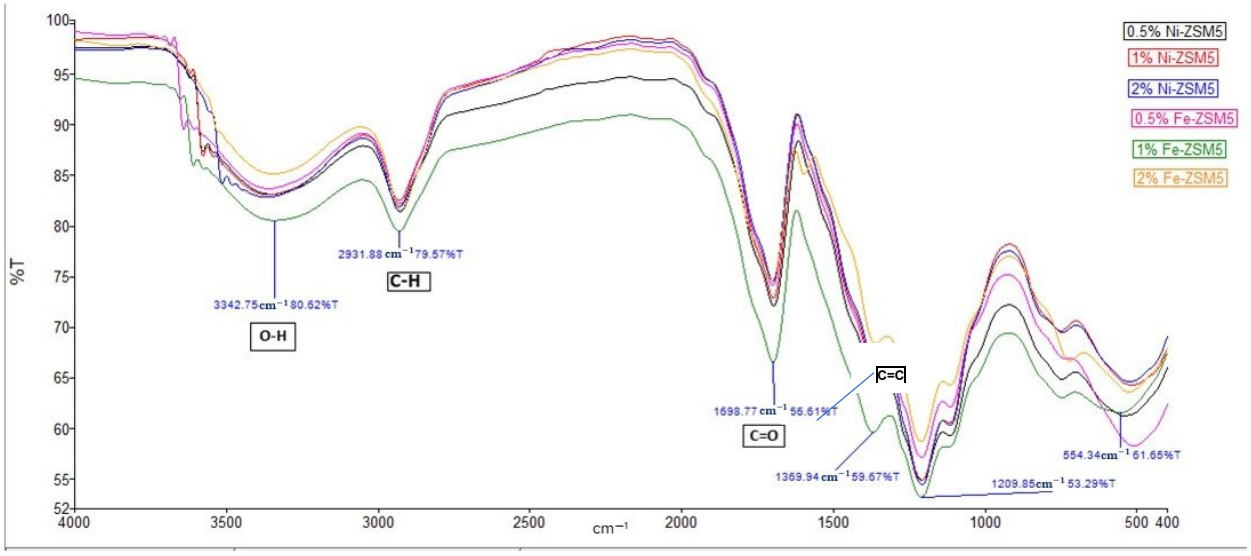

Figure 14. FTIR spectra of bio-oils obtained from the metal-doped ZSM-5 catalyst.

Vibrational bands in the 800 to 1200 cm^{-1} range, such as stretching OH, stretching H, and stretching O, probably originated from aromatics, alcohols, esters, and alkanes. Furthermore, the stretching bands at 750 cm^{-1} were attributed to the aromatic compounds present in bio-oil. Importantly, the introduction of catalysts led to a reduction in functional groups on the hydro char surface, and there was a noticeable increase in the intensity of the peak associated with the aromatic ring at 800 to 900 cm^{-1}. These findings indicate that ZSM-5 catalysts effectively facilitated the degradation of long-chain polymers into simpler organic compounds, which were later transformed into liquid products.

5. Conclusions and Recommendations

5.1. Conclusions

In summary, our comprehensive investigation of sugarcane bagasse hydrothermal liquefaction (HTL), coupled with the modification and characterisation of ZSM-5 catalysts, has yielded significant insights that advance the optimisation of process parameters and improve catalytic efficiency for bio-oil production. This research has addressed key aspects such as reaction temperature, duration, and catalyst loading, providing practical guidance for scaling up the hydrothermal liquefaction process.

The direct correlation between the quantity of sugarcane bagasse and the bio-oil yield underscores the importance of optimising the quantities of feedstock for higher efficiency. The identified optimal HTL temperature of 340 °C, coupled with a 1h duration, has proven crucial in maximising bio-oil yield while maintaining process efficiency. Furthermore, the study reveals that 30% of the ZSM-5 catalyst loading strikes a balance between catalytic effectiveness and bio-oil production. The introduction of Ni and Fe metals to ZSM-5 catalysts has shown promising results, with modified catalysts that exhibit enhanced catalytic activity without compromising the fundamental structure of the zeolite. The success of this modification is confirmed through comprehensive characterisations employing FTIR, XRD, SEM-EDS, TGA, and TEM techniques, providing detailed insights into the composition and stability of the catalysts.

The bio-oil yield obtained with the 2% Fe/ZSM-5 catalyst is significantly higher than that obtained with pure ZSM-5, suggesting that iron modification (Fe) plays a pivotal role in facilitating biomass conversion into bio-oil constituents. The increase in hydrocarbon content in bio-oil produced with modified ZSM-5 catalysts, particularly 2% Ni/ZSM-5 and 2% Fe/ZSM-5, indicates enhanced catalytic activity and holds promise for various applications, including biofuels. GC-MS analysis further delves into the detailed composition of bio-oil, revealing that the use of modified ZSM-5 catalysts leads to an increase in

hydrocarbon content and a decrease in oxygenated compounds, emphasising enhanced catalytic activity and potential applications in renewable energy sources. FTIR analysis of bio-oil provides additional insights into its molecular structure, highlighting the presence of various functional groups that contribute to its complexity.

In conclusion, this research serves as a foundation for the advancement of the field of bioenergy, providing valuable information that can inform future research and development efforts to achieve efficient and sustainable biofuel production. The optimised conditions and modified catalysts presented here pave the way for further exploration and innovation in the pursuit of renewable and environmentally friendly energy sources.

5.2. Recommendations

Based on the insights derived from this study, future research efforts in the realm of bioenergy and hydrothermal liquefaction (HTL) should be directed toward advancing catalyst design and specificity. The success achieved in the modification of ZSM-5 catalysts highlights the potential for further exploration into advanced catalysts with improved efficiency and application specificity. Researchers are encouraged to consider the development of catalysts that can address the intricate requirements of diverse biomass feedstocks, ultimately expanding the scope and versatility of HTL in renewable energy applications.

Fine-tuning process parameters emerge as a critical avenue for future investigations with a focus on optimising these parameters for different biomass sources. This approach holds promise in unlocking enhanced catalytic performance and selectivity, providing a tailored methodology for bio-oil production applications. To ensure the practicality of the modified catalysts, we should devote our attention to assessing their long-term stability and recyclability. The evaluation of the ability of these catalysts to endure prolonged use and their potential for regeneration is pivotal to their feasibility in large-scale industrial applications. Researchers are encouraged to explore downstream processing techniques to refine and upgrade bio-oil produced through HTL. Addressing challenges related to stability, viscosity, and storage will be essential to meet specifications for various applications, including transportation fuels and chemical feedstocks. Additionally, a thorough economic analysis is warranted, encompassing factors such as feedstock availability, catalyst costs, and energy consumption, to guide the optimisation of the entire process for commercialisation.

In conclusion, the recommendations of this study outline a path for future exploration and innovation in the field of bioenergy and high-temperature hybridisation. The journey toward sustainable bio-oil production beckons collaborative efforts to pursue a greener and more environmentally friendly energy future.

Author Contributions: Conceptualisation, T.J.; methodology, T.J. and N.S.S.; validation, T.J., N.S.S. and L.K.; formal analysis, T.J.; investigation, T.J.; resources, L.K.; data curation, T.J. and N.S.S.; writing—original draft preparation, T.J., N.S.S. and L.K.; writing—review and editing, N.S.S. and L.K.; visualization, T.J., N.S.S. and L.K.; supervision, N.S.S. and L.K.; project administration, L.K.; funding acquisition, L.K. All authors have read and agreed to the published version of the manuscript.

Funding: This research was funded by the National Research Foundation: 138079 and Eskom (South Africa): 2002/015527/0.

Data Availability Statement: The authors declare that the data supporting the findings of this study are available in the article.

Conflicts of Interest: The authors declare no conflicts of interest.

References

1. Musa, S.D.; Zhonghua, T.; Ibrahim, A.O.; Habib, M. China's energy status: A critical look at fossils and renewable options. *Renew. Sustain. Energy Rev.* **2018**, *81*, 2281–2290. [CrossRef]
2. Jideani, T.; Chukwuchendo, E.; Khotseng, L. An Approach towards the Conversion of Biomass Feedstocks into Biofuel Using a Zeolite Socony Mobil-5-Based Catalysts via the Hydrothermal Liquefaction Process: A Review. *Catalysts* **2023**, *13*, 1425. [CrossRef]
3. Forero, J.A.J.; Tran, T.H.T.; Tana, T.; Baker, A.; Beltramini, J.; Doherty, W.O.S.; Moghaddam, L. Hydrothermal liquefaction of sugarcane bagasse to bio-oils: Effect of liquefaction solvents on bio-oil stability. *Fuel* **2022**, *312*, 122793. [CrossRef]

4. Koçar, G.; Civaş, N. An overview of biofuels from energy crops: Current status and future prospects. *Renew. Sustain. Energy Rev.* **2013**, *28*, 900–916. [CrossRef]
5. Ravichandran, S.R.; Venkatachalam, C.D.; Sengottian, M.; Sekar, S.; Kandasamy, S.; Ramasamy Subramanian, K.P.; Purushothaman, K.; Lavanya Chandrasekaran, A.; Narayanan, M. A review on hydrothermal liquefaction of algal biomass on process parameters, purification and applications. *Fuel* **2022**, *313*, 122679. [CrossRef]
6. Purnama, I.; Trisunaryanti, W.; Wijaya, K.; Mutamima, A.; Oh, W.C.; Boukherroub, R.; Aziz, M. Multi-Pathways for Sustainable Fuel Production from Biomass Using Zirconium-Based Catalysts: A Comprehensive Review. *Energy Technol.* **2024**, *12*, 2300901. [CrossRef]
7. Nishu; Liu, R.; Rahman, M.M.; Sarker, M.; Chai, M.; Li, C.; Cai, J. A review on the catalytic pyrolysis of biomass for the bio-oil production with ZSM-5: Focus on structure. *Fuel Process. Technol.* **2020**, *199*, 106301. [CrossRef]
8. Balasundram, V.; Ibrahim, N.; Kasmani, R.M.; Isha, R.; Hamid, M.K.A.; Hasbullah, H.; Ali, R.R. Catalytic upgrading of sugarcane bagasse pyrolysis vapours over rare earth metal (Ce) loaded HZSM-5: Effect of catalyst to biomass ratio on the organic compounds in pyrolysis oil. *Appl. Energy* **2018**, *220*, 787–799. [CrossRef]
9. Kariim, I.; Swai, H.; Kivevele, T. Bio-Oil Upgrading over ZSM-5 Catalyst: A Review of Catalyst Performance and Deactivation. *Int. J. Energy Res.* **2023**, *2023*, 4776962. [CrossRef]
10. Reza, M.S.; Zhanar Baktybaevna, I.; Afroze, S.; Kuterbekov, K.; Kabyshev, A.; Bekmyrza, K.Z.; Kubenova, M.M.; Bakar, M.S.A.; Azad, A.K.; Roy, H.; et al. Influence of Catalyst on the Yield and Quality of Bio-Oil for the Catalytic Pyrolysis of Biomass: A Comprehensive Review. *Energies* **2023**, *16*, 5547. [CrossRef]
11. Nishu; Li, Y.; Liu, R. Catalytic pyrolysis of lignin over ZSM-5, alkali, and metal modified ZSM-5 at different temperatures to produce hydrocarbons. *J. Energy Inst.* **2022**, *101*, 111–121. [CrossRef]
12. Wei, Y.; Xu, D.; Xu, M.; Zheng, P.; Fan, L.; Leng, L.; Kapusta, K. Hydrothermal liquefaction of municipal sludge and its products applications. *Sci. Total Environ.* **2024**, *908*, 168177. [CrossRef]
13. Unnikrishnan, R.S.G. A novel anionic surfactant as template for the development of hierarchical ZSM-5 zeolite and its catalytic performance. *J. Porous Mater.* **2020**, *27*, 691–700. [CrossRef]
14. Saini, B.; Tathod, A.P.; Diwakar, J.; Arumugam, S.; Viswanadham, N. Corrigendum to "Nickel nano-particles confined in ZSM-5 framework as an efficient catalyst for selective hydrodeoxygenation of lignin-derived monomers" [Biomass Bioenergy 157 (2022) 106350]. *Biomass Bioenergy* **2023**, *177*, 106888. [CrossRef]
15. Sun, L.; Wang, Z.; Chen, L.; Yang, S.; Xie, X.; Gao, M.; Zhao, B.; Si, H.; Li, J.; Hua, D. Catalytic fast pyrolysis of biomass into aromatic hydrocarbons over Mo-modified ZSM-5 catalysts. *Catalysts* **2020**, *10*, 51. [CrossRef]
16. van Vreeswijk, S.H.; Weckhuysen, B.M. Emerging analytical methods to characterize zeolite-based materials. *Natl. Sci. Rev.* **2022**, *9*, nwac047. [CrossRef]
17. Cheng, Y.; Wang, L.-J.; Li, J.-S.; Yang, Y.-C.; Sun, X.-Y. Preparation and characterization of nanosized ZSM-5 zeolites in the absence of organic template. *Mater. Lett.* **2005**, *59*, 3427–3430. [CrossRef]
18. Sarve, D.T.; Singh, S.K.; Ekhe, J.D. Ethanol dehydration to diethyl ether over ZSM-5 and β-Zeolite supported Ni W catalyst. *Inorg. Chem. Commun.* **2022**, *139*, 109397. [CrossRef]
19. Chai, M.; Liu, R.; He, Y. Effects of SiO_2/Al_2O_3 ratio and Fe loading rate of Fe-modified ZSM-5 on selection of aromatics and kinetics of corn stalk catalytic pyrolysis. *Fuel Process. Technol.* **2020**, *206*, 106458. [CrossRef]
20. Daniel, S.; Karel, C.; Monguen, F.; El Kasmi, A.; Arshad, M.F. Oxidative Dehydrogenation of Propane to Olefins Promoted by Zr Modified ZSM-5. *Catal. Lett.* **2023**, *153*, 285–299. [CrossRef]
21. Cui, Y.; Chen, B.; Xu, L.; Chen, M.; Wu, C.; Qiu, J.; Cheng, G.; Wang, N.; Xu, J.; Hu, X. CO2 methanation over the Ni-based catalysts supported on the hollow ZSM-5 zeolites: Effects of the hollow structure and alkaline treatment. *Fuel* **2023**, *334*, 126783. [CrossRef]
22. Nie, P.; Liu, X.; Zhang, P.; Yuan, X.; Li, X.; Lin, S. Quaternary ammonium cellulose promoted synthesis of hollow nano-sized ZSM-5 zeolite as stable catalyst for benzene alkylation with ethanol. *J. Mater. Sci.* **2021**, *56*, 8461–8478. [CrossRef]
23. Anekwe, I.M.S.; Chetty, M.; Khotseng, L.; Kiambi, S.L.; Maharaj, L.; Oboirien, B.; Isa, Y.M. Stability, deactivation and regeneration study of a newly developed HZSM-5 and Ni-doped HZSM-5 zeolite catalysts for ethanol-to-hydrocarbon conversion. *Catal. Commun.* **2024**, *186*, 106802. [CrossRef]
24. Sudarsanam, P.; Peeters, E.; Makshina, E.V.; Parvulescu, V.I.; Sels, B.F. Advances in porous and nanoscale catalysts for viable biomass conversion. *Chem. Soc. Rev.* **2019**, *48*, 2366–2421. [CrossRef]
25. Fu, T.; Chang, J.; Shao, J.; Li, Z. Fabrication of a nano-sized ZSM-5 zeolite with intercrystalline mesopores for conversion of methanol to gasoline. *J. Energy Chem.* **2017**, *26*, 139–146. [CrossRef]
26. Da Silva, L.S.; Araki, C.A.; Marcucci, S.M.P.; da Silva, V.L.D.S.T.; Arroyo, P.A. Desilication of ZSM-5 and ZSM-12 zeolites with different crystal sizes: Effect on acidity and mesoporous initiation. *Mater. Res.* **2019**, *22*, 15879–15886. [CrossRef]
27. Peron, D.V.; Zholobenko, V.L.; de la Rocha, M.R.; Oberson de Souza, M.; Feris, L.A.; Marcilio, N.R.; Ordomsky, V.V.; Khodakov, A.Y. Nickel–zeolite composite catalysts with metal nanoparticles selectively encapsulated in the zeolite micropores. *J. Mater. Sci.* **2019**, *54*, 5399–5411. [CrossRef]
28. Sabarish, R.; Unnikrishnan, G. Synthesis, characterization and evaluations of micro/mesoporous ZSM-5 zeolite using starch as bio template. *SN Appl. Sci.* **2019**, *1*, 989. [CrossRef]

29. Widayat, W.; Annisa, A.N. Synthesis and Characterization of ZSM-5 Catalyst at Different Temperatures. *IOP Conf. Ser. Mater. Sci. Eng.* **2017**, *214*, 012032. [CrossRef]
30. Nagappan, S.; Bhosale, R.R.; Duc, D.; Thuy, N.; Chi, L. Catalytic hydrothermal liquefaction of biomass into bio-oils and other value- added products—A review. *Fuel* **2021**, *285*, 119053. [CrossRef]
31. Makhado, T. Hydrothermal Conversion of Agricultural and Food Waste. 2022. Available online: https://etd.uwc.ac.za/xmlui/bitstream/handle/11394/9087/makhado_m_nsc_2022.pdf?sequence=1&isAllowed=y (accessed on 14 September 2024).
32. Deng, W.; Feng, Y.; Fu, J.; Guo, H.; Guo, Y.; Han, B.; Jiang, Z.; Kong, L.; Li, C.; Liu, H.; et al. ScienceDirect Catalytic conversion of lignocellulosic biomass into chemicals and fuels. *Green Energy Environ.* **2023**, *8*, 110–114. [CrossRef]
33. Masfuri, I.; Amrullah, A.; Farobie, O.; Anggoro, T.; Rain, S.F.; Prabowo, W.; Rosyadi, E. Results in Engineering Temperature effects on chemical reactions and product yields in the Co-pyrolysis of wood sawdust and waste tires: An experimental investigation. *Results Eng.* **2024**, *23*, 102638. [CrossRef]